12-2019

A Synthesis and Analysis of Anhydrous Hydroxide Ion Conducting Polymer Electrolytes

Stanton Heydinger

Recommended Citation

Heydinger, Stanton, "A Synthesis and Analysis of Anhydrous Hydroxide Ion Conducting Polymer Electrolytes" (2019). *Honors Theses*. 1558.
https://egrove.olemiss.edu/hon_thesis/1558

A SYNTHESIS AND ANALYSIS OF ANHYDROUS HYDROXIDE ION CONDUCTING POLYMER ELECTROLYTES

by
Stanton Paul Heydinger

A thesis submitted to the faculty of the University of Mississippi in partial fulfillment of the requirements of the Sally McDonnell Barksdale Honors College.

Oxford
May 2019

Approved by:

Advisor: Dr. Jason Ritchie

Reader: Dr. Jonah Jurss

Reader: Dr. Nathan Hammer

DEDICATION

To my grandparents Richard and Sandra Heydinger who have supported me endlessly throughout every step of my life.

ACKNOWLEDGEMENTS

First, I would like to thank my parents Edith and Matthew Heydinger, and my sister Madison Heydinger for supporting me throughout my academic career. Without the financial and emotional support, I would not have been able to complete this project. Throughout my time at the University of Mississippi several people have relentlessly supported me in every endeavor and challenged me to become a better student and person. Thank you to all of you unnamed individuals who have continually pushed me and kept me focused. I would also like to thank Dr. Jason Ritchie for his invaluable input, patience, and guidance throughout the course of this research. Additionally, I would like to thank the Sally McDonnell Barksdale Honors College for the incredible opportunities they have afforded me throughout my time at the University.

ABSTRACT

This project investigates the synthesis and physical properties of polyethylene glycol monomethyl ether ($MePEG_n$ where n=3 or 7) based polymer electrolytes. The two polymer electrolytes explored in the experiments were designed from two different MePEG chains that varied in their overall length and degree of polymerization. The first MePEG backbone contained three polymerized ethoxy groups and the second contained seven. Both $MePEG_n$ polymers were modified by substituting an imidazolium group in place of the alcohol functional group at the end of the PEG chain. This modification was made to create a polymer electrolyte with an attached positive charge that could facilitate the movement of hydroxide ions. These polymer electrolytes were synthesized in order to study various physical properties, such as ionic conductivity and viscosity, in anhydrous conditions to characterize the viability of the MePEG derivatives as alkaline anion exchange membrane fuel cells (AAEMFCs) polymer electrolyte membranes.

TABLE OF CONTENTS

LIST OF ABBREVIATIONS

PEG 350	Poly (ethylene glycol), Molecular Weight 350
PEG 750	Poly (ethylene glycol), Molecular Weight 750
$MePEG_nOH$	Polyethylene Glycol Monomethyl Ether
η	Viscosity
S	Siemens
NMR	Nuclear Magnetic Resonance Spectroscopy
σ	Conductivity
Λ	Molar Equivalent Conductivity
$CH_3SO_3^-$	Methanesulfonate Ion (Mesylate)
IM	Imidazolium Group
OH^-	Hydroxide Ion
cP	Centipoise
K	Kelvin
k	Boltzmann Constant
T	Absolute Temperature
R	Hydrodynamic Radius of the Particle
k	Boltzmann Constant
E_a	Activation Energy
z	Charge of the Particle
D	Diffusion Coefficient
C	Concentration

F	Faraday Constant

LIST OF FIGURES

INTRODUCTION

Fuel cells are electrochemical devices that can directly convert chemical energy into electricity. An exciting alternative fuel source, fuel cells are remarkable for their clean production of energy using fairly simple reactions. The most commonly exploited reaction to power a fuel cell is the combination of hydrogen and oxygen to form water.

$$2\ H_2\ (g) + O_2\ (g) \rightarrow 2\ H_2O\ (l) \qquad E_0 = +1.23V$$

Through combining these two molecules in a closed system, the cell is able to generate a usable form of energy (electricity) while the only by product is water. Fuel cells can be used as power sources for a wide range of applications, such as transportation or residential power and are a viable alternative to combustion engines and batteries. The key issues impeding the common adoption of fuel cells are: combatting the need for expensive, rare-earth electrocatalysts that facilitate these simple reactions, generating hydrogen from renewable sources, creating a hydrogen infrastructure, and improving the overall efficiency of fuel cells to enable their operation at higher temperatures to be more tolerant of carbon monoxide in the hydrogen fuel stream. In order to operate at higher temperatures, the fuel cell electrolyte will have to be more capable of conducting H^+ ions at much lower water concentrations. Thus, we have been developing new membrane materials that conduct ions without water.

The most common catalyst used in fuel cells currently is the expensive transition metal, platinum. With the current cost of platinum being well-over twenty thousand dollars per kilogram, it is apparent that there is a need for a cheaper alternative. In order to substitute a less expensive catalyst material, fuel cell efficiency must be improved at higher temperatures. One method to improve the high temperature efficiency is to improve conductivity of the electrolyte at low water concentrations.

The most studied form of polymer electrolyte fuel cells is the proton exchange membrane fuel cell (PEMFC). Proton exchange membrane fuel cells use an acidic polymer membrane as its electrolyte with platinum-based electrodes. The polymer membrane electrolyte has the responsibility of conducting hydrogen cations (H^+) from the anode to the cathode. Nafion, is a widely used commercial polymer electrolyte that has good chemical stability and high conductivity when wet. The main drawback with this type of electrolyte is the cost of the fuel cell due to the need to incorporate a noble-metal catalyst, usually platinum.

Another type of fuel cell architecture is the alkaline fuel cell (AFC). In these hydroxide ion conducting fuel cells, the most common electrolyte that has been used is a solution of potassium hydroxide in water in the Alkaline Fuel Cell geometry (AFC). This solution offers high efficiency, especially for the Oxygen Reduction Reaction (ORR) at the cathode, but requires a purified oxygen stream and has the potential of leaking a highly caustic liquid. In addition, alkaline fuel cells using potassium hydroxide electrolytes tend to precipitate carbonates on the electrodes when exposed to air (e.g. to provide oxygen for the cathode reaction). These byproducts are introduced into the system from atmospheric carbon dioxide reacting with the strongly basic electrolyte.

$$OH^- + CO_2 \rightleftharpoons HCO_3^-$$

$$OH^- + HCO_3^- \rightleftharpoons CO_3^{2-} + H_2O$$

Figure 1. Formation of carbonate precipitant in alkaline conditions

The extremely basic electrolyte absorbs any carbon dioxide introduced to the system, which leads to precipitation of sodium carbonate in the basic medium, and a reduction in conductivity due to the increasing presence of solid material in the conduction pathway. To avoid facing these issues, Alkaline Fuel Cells typically use pure oxygen (instead of air) which leads to a significant increase in cost. Most fuel cell architectures make use of air at the cathode as a source of oxygen. Despite these issues, early alkaline fuel cells using liquid electrolyte have been used to power space crafts during the Apollo and Space Shuttle space missions, where pure oxygen would already be available. To increase the potential uses of Alkaline Fuel Cells the durability and chemical stability needs to increase. One way to attempt to achieve these goals is to use a polymer based electrolyte.

Alkaline anion exchange membrane fuel cells (AAEMFCs) use a polymer electrolyte to separate the anode from the cathode within a fuel cell and conduct hydroxide ions (OH-) between the two electrodes. In addition, these electrolyte membranes have the potential to block the absorption of CO_2 into the alkaline electrolyte allowing the fuel cell to breath air as a source of oxygen. At the cathode, the reduction of oxygen molecules produces hydroxide ions that move through the electrolyte towards the anode. At the anode, hydrogen gas is oxidized to release electrons and protons that react with the hydroxide ions to form water. These electrons move through a circuit to produce a current and generate electricity that can be harnessed for work. The main advantage of using an Anion Exchange Membrane is the improved efficiency of the oxygen reduction reaction (ORR) while in an alkaline environment. This improvement could potentially lead to the use of less expensive, non-platinum group metal catalysts.

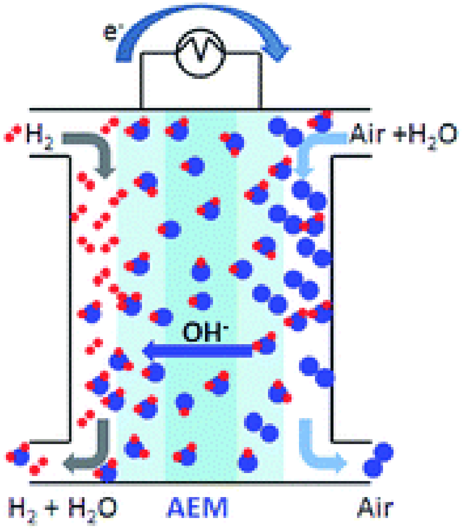

$$O_2\,(g) + 2\,H_2O\,(l) + 4\,e^- \rightarrow 4\,OH^-\,(aq) \qquad E_0 = +0.401\text{ V vs S.H.E}$$

$$2\,H_2 + 4\,OH^-\,(g) \rightarrow 4\,H_2O\,(l) + 4\,e^- \qquad E_0 = -0.8277\text{ V vs S.H.E}$$

$$2\,H_2\,(g) + O_2\,(g) \rightarrow 2\,H_2O\,(l) \qquad E_{0cell} = +1.23\text{ V}$$

Figure 2. Hydroxide-Conducting Fuel Cell (AAEMFC). Figure adapted from Reference.[1]

The polymer electrolyte we are exploring consists of a polymer backbone with a covalently-attached cationic group to assist in the movement of free hydroxide ions. These electrolytes must have a high degree of ionic conductivity and chemical stability to function as an AAEMFC electrolyte. The study of AAEMFCs is fairly new and relatively unexplored, as proton exchange membranes were more thoroughly explored earlier. Thus, there is not a lot of experimental data for anion conducting polymer electrolytes that has been reported in the chemical literature. In this project, we have studied the synthesis, ion transport, and viscoelastic properties of the MePEG-based, hydroxide-ion conducting polymer electrolyte.

In order to test the physical property of ionic conductivity, we used AC-impedance spectroscopy using an Electrochemical Potentiostat (PAR Model 283) and a lock-in amplifier. Conductivity (Siemens/cm) is the ability of a material to allow ions to diffuse through it. Conductivity is the inverse value of resistivity (ohm•cm), which is a temperature-dependent property, that is also dependent on the mechanism of the ionic conduction through the material.

The conductivity of our polymer electrolyte samples was measured using AC-impedance spectroscopy on standardized conductivity electrodes. This "spectroscopic" method applies an alternating-current potential and measures the phase and magnitude of the current response through the sample to determine the real and imaginary components of impedance through the material. Resistance is the real component of impedance within the electric circuit that manifests from the opposition to a current under an applied voltage. We are primarily using this experimental method to measure the resistance in a sample, while being able to separate the resistance of the material from the capacitances that arise from electrical contact with the electrolyte material, and the double layer capacitance formed at the electrode interface. This comparison, as a function of the applied frequency, can be shown graphically with a Nyquist plot (Figure 3).

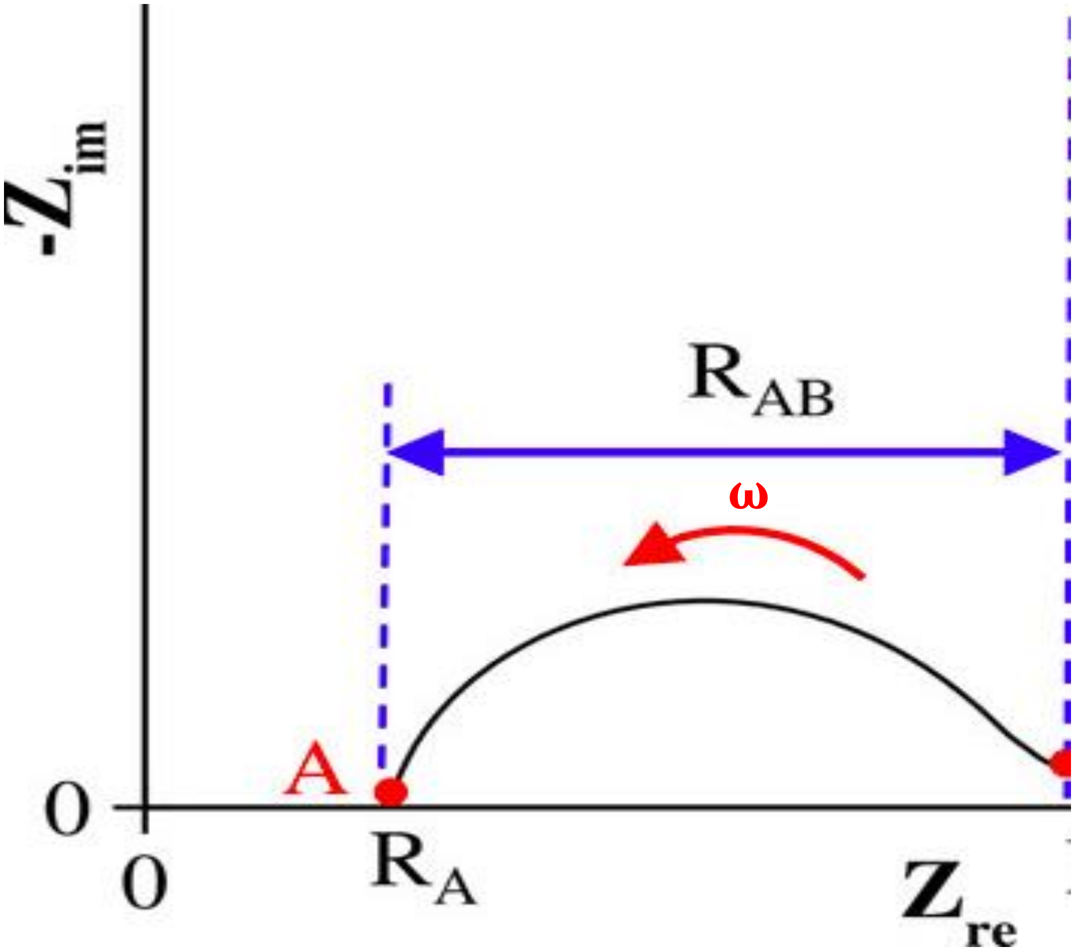

Figure 3. Typical Nyquist plot for conductivity where R_{AB} is the measured bulk resistance. Figure adapted from Reference.[2]

From a system with no Faradaic current (i.e. a pure ion conductor), the typical Nyquist plot forms the shape of a half circle at high frequencies, where the measured diameter, represented by R_{AB} in Figure 3, and is the real (x-axis) component of impedance, is the bulk resistance of the material. The Z_{im} shown on the y-axis of the graph is representative of the capacitance of the sample, because this is the component of the current response that is 90° out-of-phase with the applied voltage (i.e. capacitance). While the Z_{re} shown on the x-axis represents the component of the impedance that is in-phase with the applied voltage, and corresponds to the resistance.

By taking the reciprocal value of the diameter (conductance is measured in Siemens = ohm^{-1}) and dividing by an experimentally determined geometric factor for the electrode, the ionic conductivity can be calculated. The geometric factor of the electrode was determined experimentally before measurements had been taken by calibration with low conductivity standards.[3]

Conductivity has the units of Siemens per centimeter (S/cm). The ionic conductivity was measured at varying temperatures and these values were compared on an activation plot. By taking the logarithm of conductivity and graphing it against the inverse of the temperature, an Arrhenius activation plot can be constructed. The slope of this plot yields the activation energy for the ionic transport process.

Another commonly used unit of ionic mobility is the molar equivalent conductivity (Λ), which can be calculated by dividing the measured conductivity (S/cm) by the ionic concentration (mol/cm^3) of the polymer electrolyte. The molar equivalent conductivity allows for an easier comparison of the actual ionic mobility in solutions that are different concentrations, or are different polymers.

To determine the viscosity and fluidity of the material, a Rheometer instrument was used (Brookfield DV-III rheometer with cone and plate geometry). The cone and plate method is used to measure shear stress between two surfaces. Viscosity is the physical property of a liquid to resist flow due to shear stress. This property is temperature dependent and typically increases with temperature.[4] To take measurements, the liquid is placed in a plate and a shallow cone is rotated across the surface. Different cones can be used to measure viscosity depending on how viscous a material is. For our experiments, a CPE-40 cone was used. Viscosity is measured in poise (P) or centipoise (cP) and fluidity is the reciprocal of viscosity (fluidity = viscosity^{-1}).

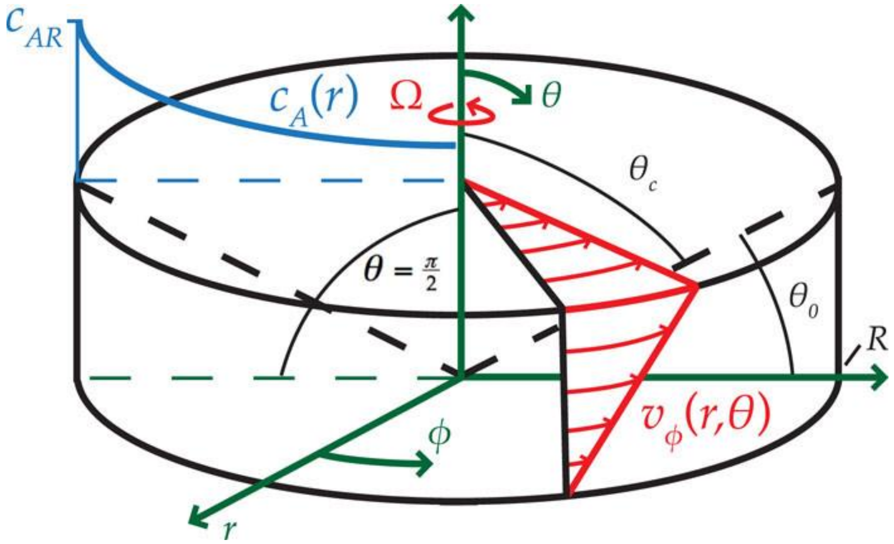

Figure 4. Cone and Plate Rheometer setup defining spherical coordinates and boundaries. Figure Adapted from Reference.[5]

EXPERIMENTAL

Polymer Electrolyte Synthesis

Both polymers used in these experiments were synthesized in the lab starting with a polyethylene glycol monomethyl ether backbone ($Me(PEG)_nOH$).

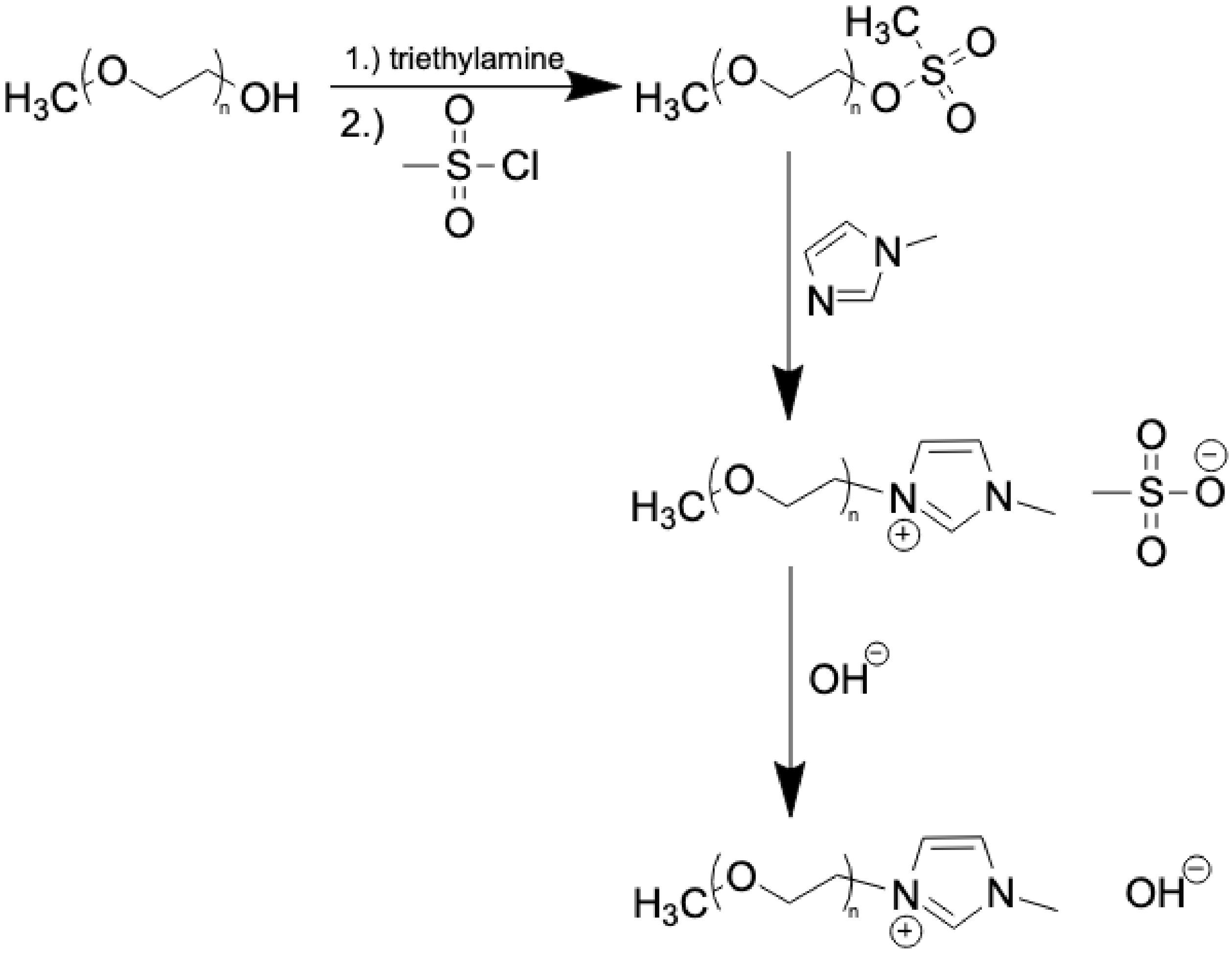

Scheme 1: Synthesis of $MePEG_nIm^+ OH^-$

Synthesis of MePEG$_3$-mesylate

Monomethyl polyethylene glycol MW = 164 g/mol (20.0 g, 0.122 mol) was mixed with triethylamine ($C_6H_{15}N$, 12.32 g, 0.122 mol) in an Erlenmeyer flask that was subsequently cooled in an ice bath. Methanesulfonyl chloride (CH_3SO_2Cl, 13.98 g, 0.122 mol) was added into the solution drop-wise with stirring while in the ice bath. The solution was then capped and allowed to stir in the ice bath for two hours.

Figure 5. General structure of the polyethylene glycol monomethyl ether. Monomethyl polyethylene glycol (MW = 164 g/mol) has a n-value of 3.

The reaction mixture was extracted with water and dichloromethane (CH_2Cl_2) and then moved to a separatory funnel, and allowed to separate into two layers. The less dense aqueous layer was retained and extracted twice more with 40 ml dichloromethane, and the organic fractions were combined and dried with 2 grams of anhydrous sodium sulfate (Na_2SO_4). The product was recovered by rotary evaporation yielding 17.322 g (58.6% yield).

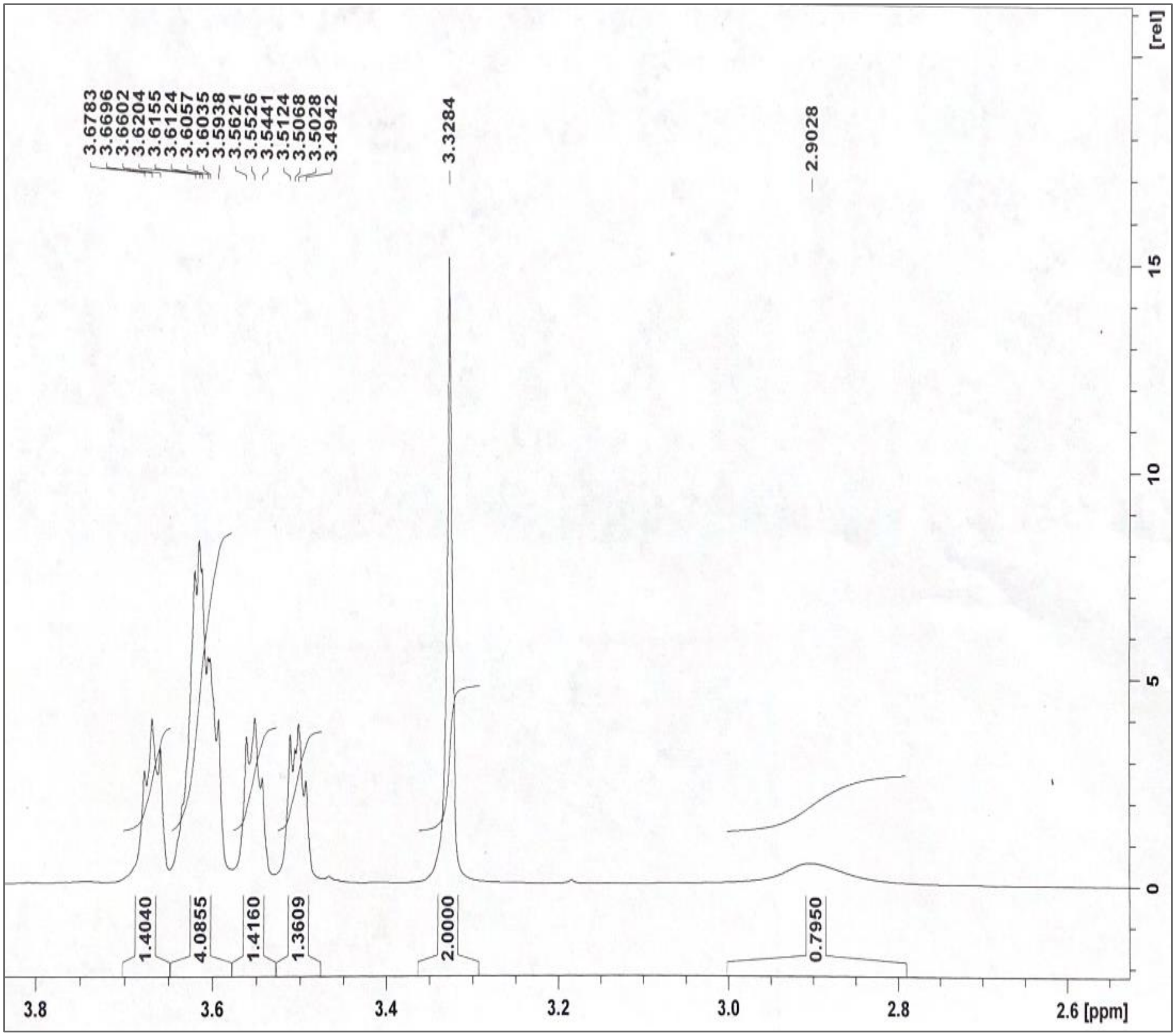

Figure 6. ^{1}H NMR Spectrum of Me(PEG)$_3$OH.

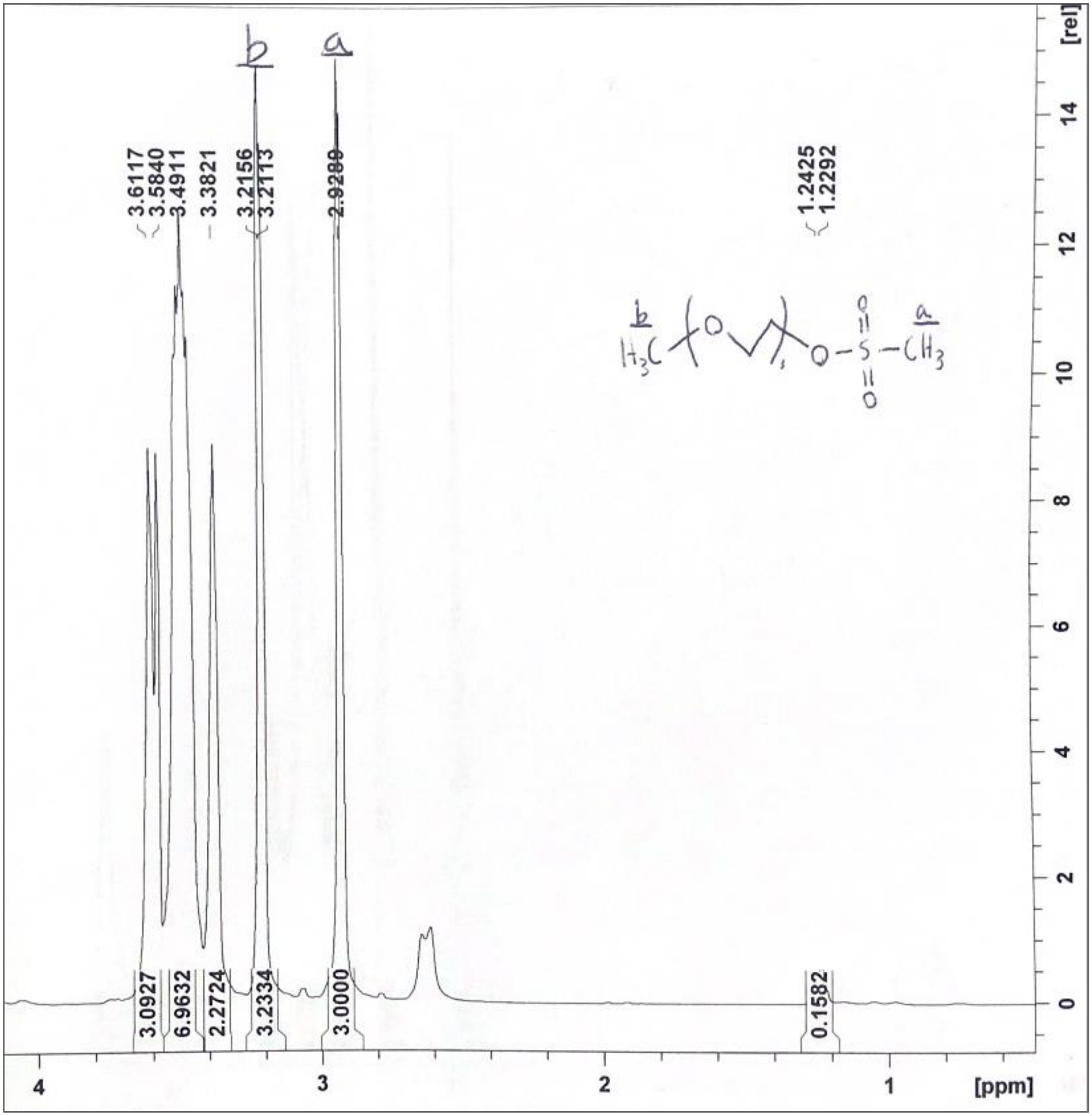

Figure 7. ^{1}H NMR Spectra of Me(PEG)$_3$–mesylate.

The result of this reaction was the conversion of the alcohol group (MePEG–OH) to a methanesulfonate substituent (MePEG–OSO_2CH_3), also referred to as a mesylate. The mesylate group is a phenomenal leaving group and was placed on the polymer chain to facilitate nucleophilic substitution of the mesylate to give an imidazole substituent in the next synthetic step. The result of this synthesis was confirmed using ^{1}H NMR, and comparing the signals and integrations of the newly added R–$OSO_2C\underline{H}_3$ hydrogens to the methyl hydrogens on the polyether portion of the polymer backbone **Me**PEG–OSO_2CH_3.

Comparing Figure 6 and Figure 7, a new singlet peak appears at 2.93 ppm. This peak is assigned to the three methyl hydrogens of the mesylate substituent. In fact, the integration of the two methyl peaks gives a 3.23:3 ratio (93%) of the peak areas which is very close to the ideal (3:3 or 100%) ratio, confirming that this reaction has essentially gone to completion.

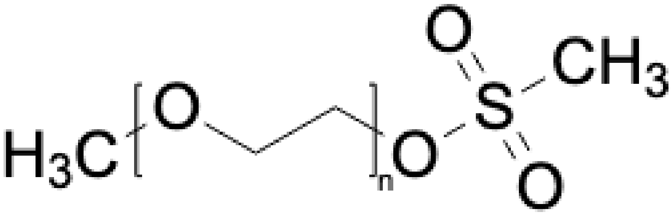

Figure 8. Structure of Mesylated MePEG.

Synthesis of $MePEG_3$-Imidazolium$^+$ $CH_3SO_3^-$

In the second step of this synthesis, the $MePEG_3$–mesylate ($MePEG_3OSO_2CH_3$,17.32 g, 0.0715 mol) was combined with 1-methylimidazole ($C_4H_6N_2$, 5.87 g, 0.0715 mol) at a one-to-one mole ratio in an external water bath kept at room temperature. This solution was allowed to stir for twenty-four hours.

This addition of the substituent was confirmed by ^1H NMR comparing the N-methyl group of the imidazole to the PEG-methyl in the original polymer backbone, once again looking for a one-to-one peak area ratio. A near one-to-one peak area ratio was obtained from the spectra. Comparing Figure 7 and Figure 9, a new singlet peak appears at 3.44 ppm. The integration of the two methyl peaks gives a 3.75:4.34 ratio (87%) which is very close to the ideal (3:3 or 100%) ratio. Another indication of successful attachment of the imidazole group was the gain of three aromatic hydrogen peaks observed from 7.0 ppm to 8.2 ppm. These hydrogens corresponded to the letters b, c, and d on the labeled imidazole ring on the spectrum. All three of these peaks gave nearly the same integration value due to each carbon in the imidazole ring being unsaturated and having one hydrogen attached.

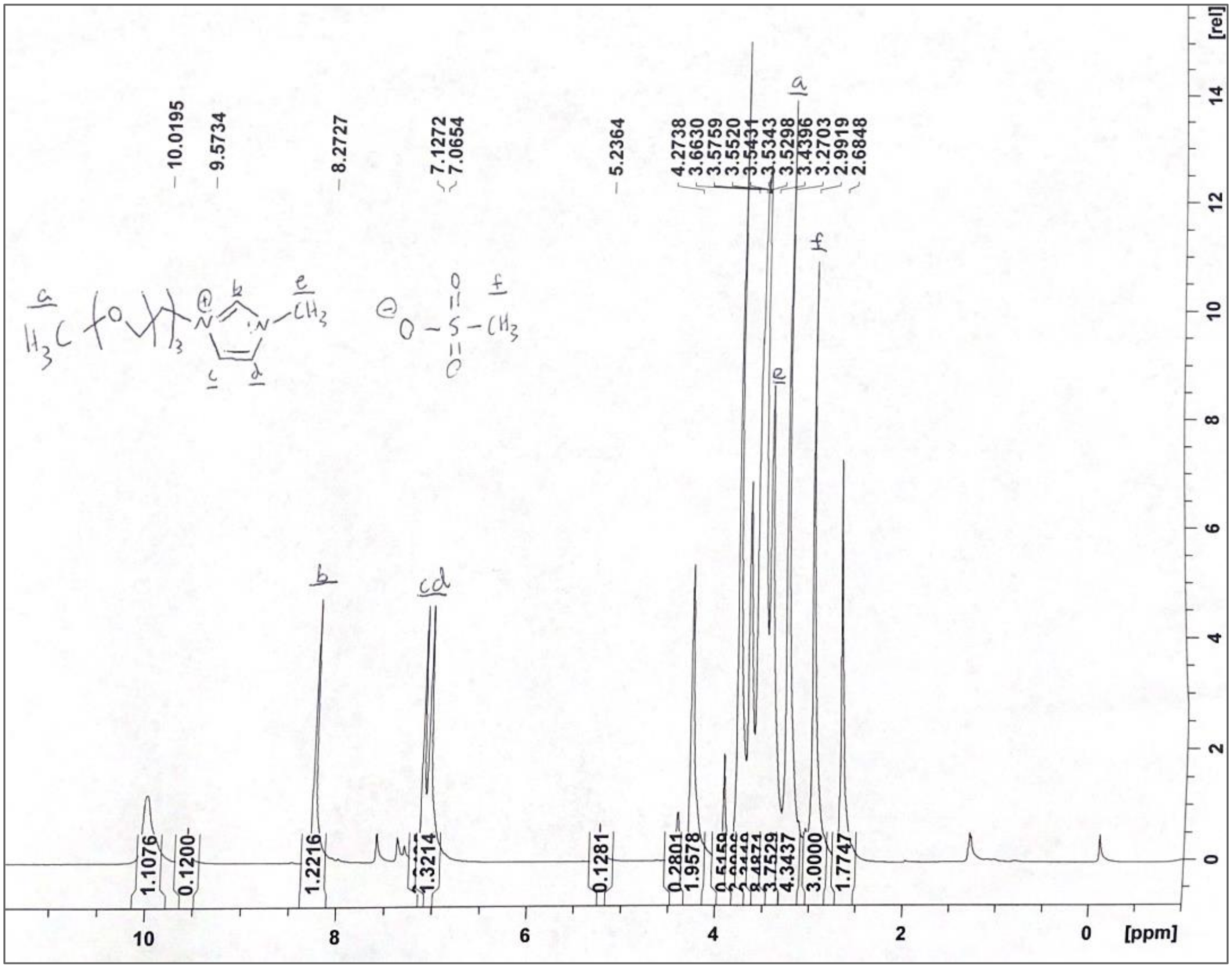

Figure 9. NMR Spectra of Me(PEG)3Imidazole

The addition of the imidazole group on the polymer backbone created a positively-charged, and covalently-attached, imidazolium group, which requires a negatively-charged counter-ion. Immediately after the second step, the counter-ion in solution was methanesulfonate ($CH_3SO_3^-$). In the next step of the synthesis, the methanesulfonate ion was ion-exchanged for the hydroxide anion (OH^-).

Ion exchange of MePEG$_n$–Imidazolium$^+$ methanesulfonate$^-$ (MePEG$_3$-Imidazolium$^+$ $CH_3SO_3^-$) to MePEG$_n$–Imidazolium$^+$ hydroxide$^-$ (MePEG-Im$^+$ OH$^-$)

The methanesulfonate counter ion ($CH_3SO_3^-$) of the previous product, MePEG$_n$–Im$^+$, was ion-exchanged from a methanesulfonate ($CH_3SO_3^-$) ion to a hydroxide (OH^-) ion using an anion exchange resin column. In order to exchange the negatively-charged counter-ions, a strongly basic exchange column was used. The column was filled with 160 mL of Amberlite IRA-400 chloride-form, strongly-basic ion exchange resin. After rinsing the column and resin with nanopure water, the column was charged with 150 mL of 4.0 M solution of sodium hydroxide (NaOH), and then rinsed with nanopure water until the pH was around 8.0.

The MePEG$_n$–Im$^+$ $CH_3SO_3^-$ obtained from the previous step was slowly run through the column as a solution in water, and then rinsed with nanopure water until the pH of the effluent was back to around 8.0. The original eluent and rinse eluent were combined into one large fraction of water solution. Getting the column back to a more neutral pH ensured that all of the MePEG$_n$Im$^+$ OH^- product had been completely eluted through the column. Ethanol was then added to the combined eluent to reduce the boiling point and the ethanol/water solvent was removed by rotary evaporation at 70 °C for about 2 hours.

To assay the effectiveness of the ion-exchange step, a small amount (100 mg) of MePEG$_n$Im$^+$ OH^- product was titrated with a 0.0153 M solution of methanesulfonic acid to the equivalent point at a pH of 7.00. The solution was titrated to an equivalent point pH of 7.00 because it was a strong acid-strong base titration.

By converting the volume of acid added to reach the equivalence point (22.8 mL) to moles, we determined that the ratio of OH^- to $MePEG_n$ was 86% indicating a successful exchange of the $CH_3SO_3^-$ ion for the hydroxide ion.

After these steps, the polymer electrolyte, methyl-poly(ethylene-1-methylimidazolium) hydroxide ($MePEG_n$–Im^+ OH^-], had been synthesized to completion. This synthesis was completed using $MePEG_3OH$ and $MePEG_7OH$, commonly referred to as mPEG three and seven, as the polymer backbone.

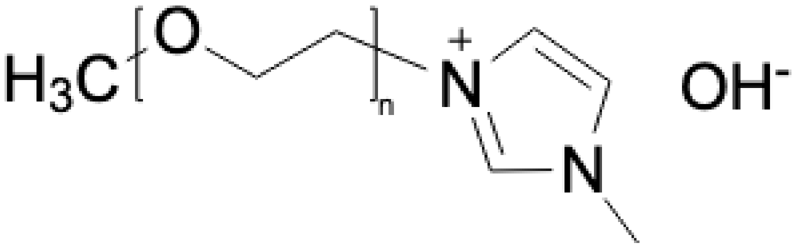

Figure 10. Structure of MePEG–methylimidazolium hydroxide.

Conductivity Measurements

The conductivity measurements were performed using a PAR 283 potentiostat equipped with a Perkin-Elmer 5210 lock-in amplifier. All trials were run in a Faraday cage to shield the sample from outside electromagnetic fields. Before experiments with the polymers began, the geometrical constant of the measuring electrode was determined to be 0.0121 using a KCl solution.[6,7] Dried, degassed samples of the $MePEG_n$–Im^+ OH^- polymer electrolytes were applied onto an electrode and sealed upright in a vacuum cell connected to a vacuum pump and temperature controlled water circulator.

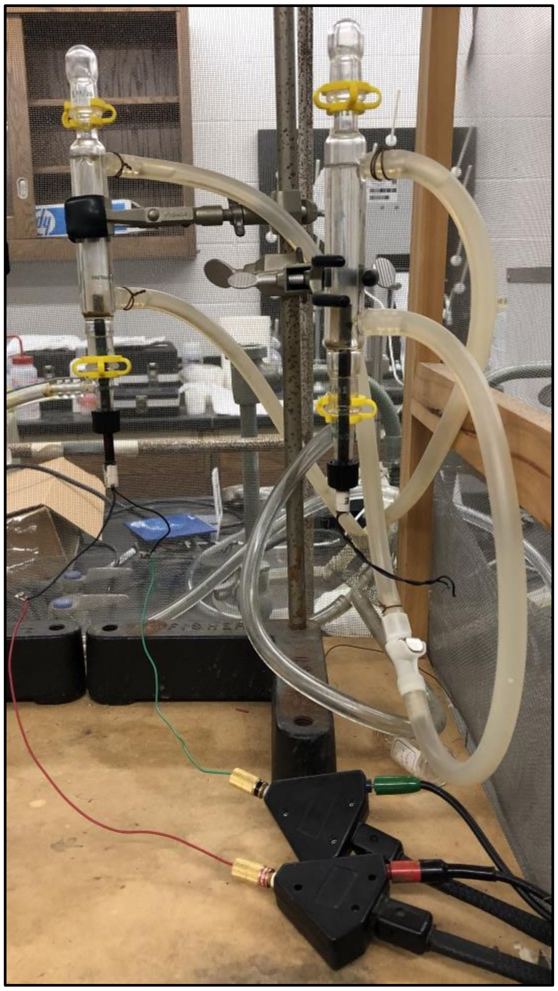

Figure 11. Setup for conductivity trials with custom built electrodes in a Faraday cage.

The trials were run from 1 kHz to 100 KHz frequencies. Each measurement was obtained through multiple trials to ensure that the sample was completely dry. If the sample was not dry, this could affect the conductivity values. The conductivity values were obtained from a Nyquist plot generated in the computer program Power Suite. On the Nyquist plot, high frequency semicircles were generated from the AC-impedance data and the diameter of the semicircle was taken as the bulk resistance of the material. By taking the inverse of the resistance and dividing by the geometrical factor for the electrode, the conductivity was calculated.

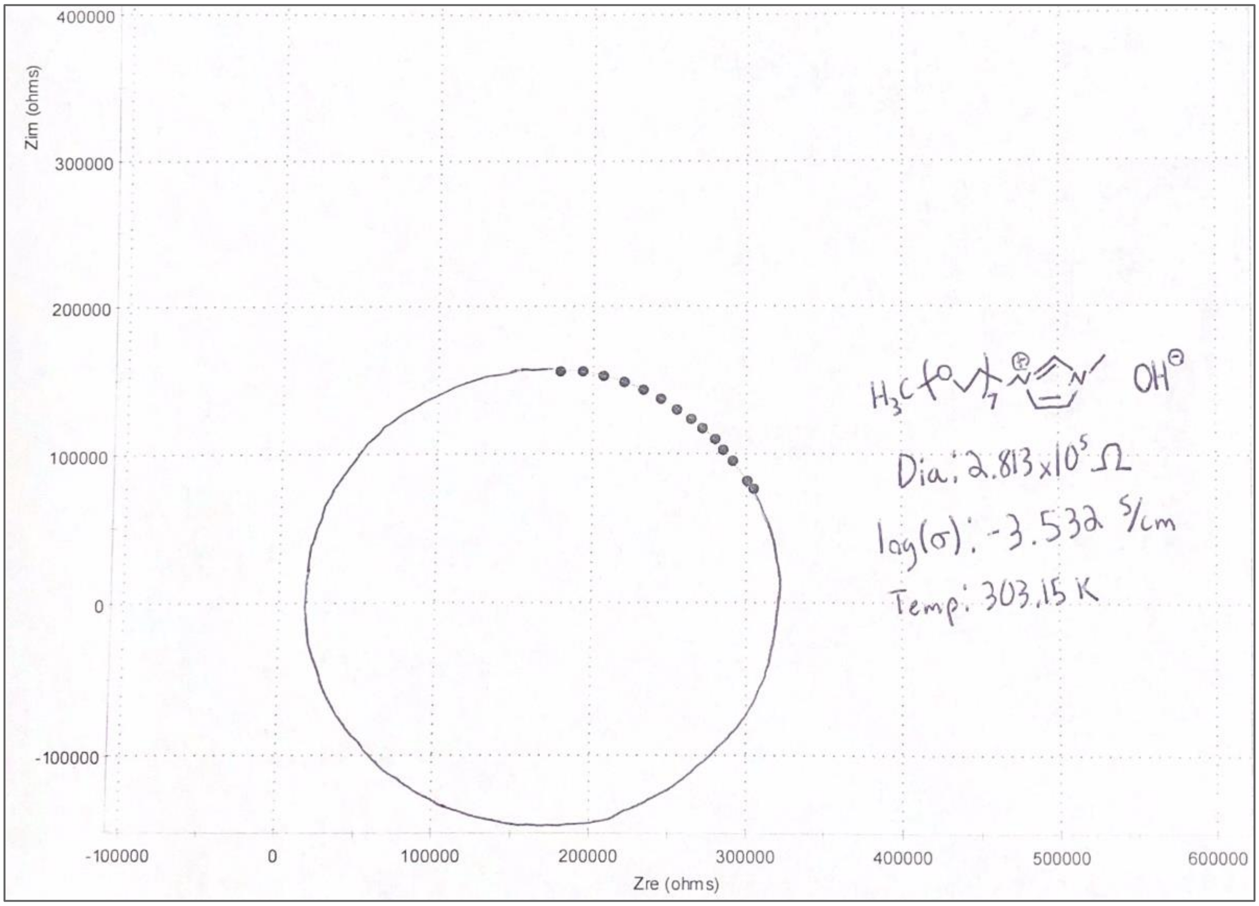

Dia: $2.813 \times 10^5\ \Omega$

log(σ): -3.532 S/cm

Temp: 303.15 K

Figure 12. Nyquist Plot of Me(PEG)$_7$-IM taken at 303.15 Kelvin.

$$(281300\ \text{ohm})^{-1} = 3.555 \times 10^{-6}\ \text{S}$$
$$3.555 \times 10^{-6}\ \text{S} / 0.0121\ \text{cm} = 2.938 \times 10^{-4}\ \text{S/cm}$$
$$\log(2.938 \times 10^{-4}) = -3.532$$

Figure 13. Calculating the log (σ) from the diameter of the Nyquist plot in Figure 12.

Conductivity measurements were obtained at 10°C increments between 10-90° Celsius, as shown in Figure 14. By taking the logarithm of the conductivity values, the results were graphed against the inverse of the temperature to give an Arrhenius activation plot for ionic conductivity. From the Arrhenius plot, the activation energy for the ionic conductivity process could be determined by finding the slope of the line.

Temperature (℃)	**PEG-3 (S/cm)**	**PEG-7 (S/cm)**
10	4.036 x 10^{-5}	1.086 x 10^{-4}
20	7.096 x 10^{-5}	1.811 x 10^{-4}
30	1.442 x 10^{-4}	2.938 x 10^{-4}
40	2.028 x 10^{-4}	3.882 x 10^{-4}
50	3.357 x 10^{-4}	6.026 x 10^{-4}
60	4.550 x 10^{-4}	1.125 x 10^{-3}
70	7.516 x 10^{-4}	1.710 x 10^{-3}
80	1.600 x 10^{-3}	5.176 x 10^{-3}
90	**3.750 x 10^{-3}**	**7.464 x 10^{-3}**

Figure 14. Conductivity Measurements for MePeg Imidazolium Polymers. The largest conductivity values were measured at 90 °C.

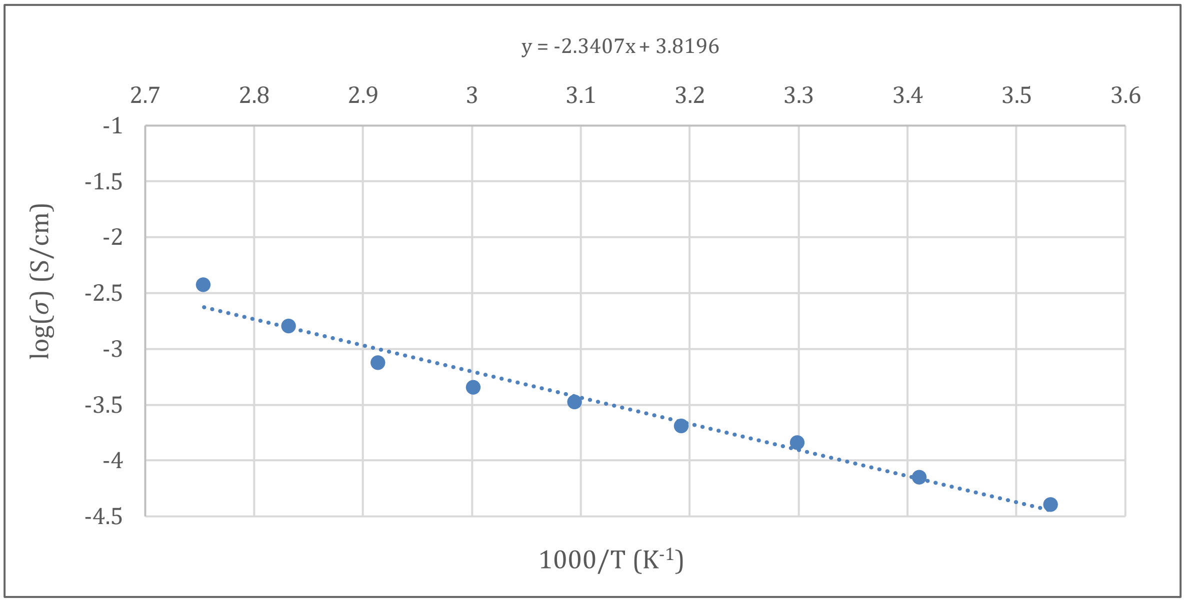

Figure 15. Arrhenius Activation Plot for MePeg3 Imidazolium, best fit line shown. The slope yielded an activation energy of 44.82 kJ/mol.

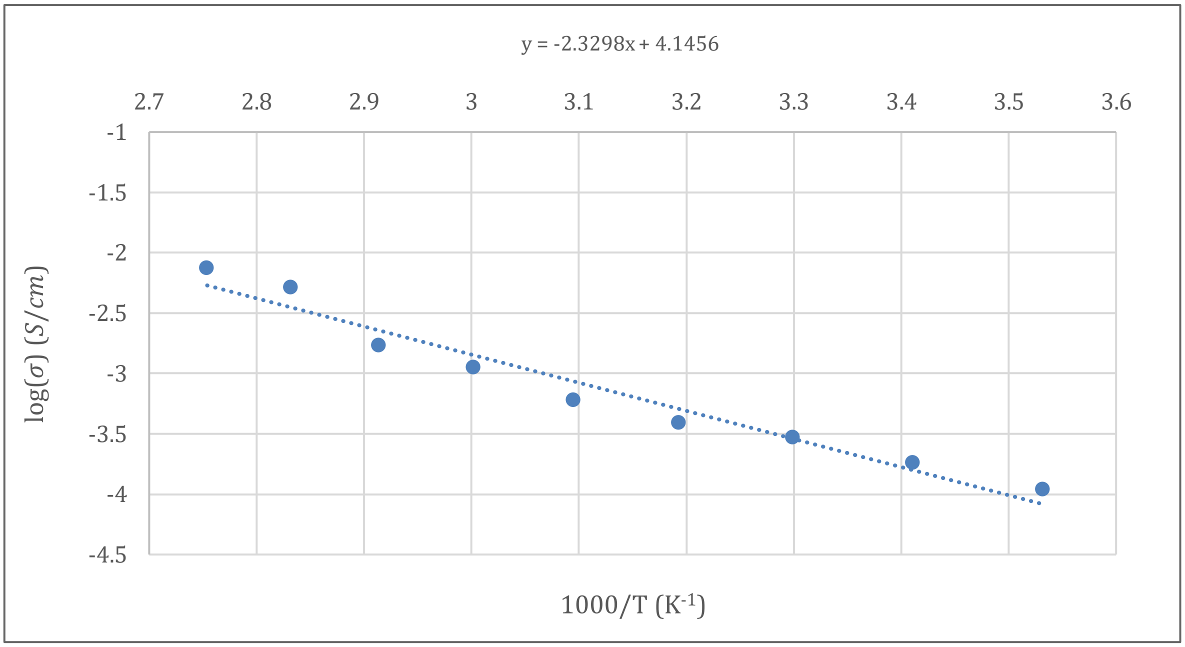

Figure 16. Arrhenius Activation Plot for MePEG$_7$–Imidazolium$^+$ OH$^-$ polymer electrolyte, best fit line shown. The slope yielded an activation energy of 44.61 kJ/mol.

Viscosity Measurements

The viscosity measurements were obtained using a Brookfield DV-III Ultra Rheometer. The sample was measured using a CPE-40 cone and connected to a closed-loop water temperature regulator. Sample viscosity was measured from 10-90° Celsius in increments of 10° Celsius. Viscosity was measured by this instrument in centipoise (cP). The specific rheometer technique used for these measurements was cone and plate. Cone and plate viscometers are used to measure viscosity of non-Newtonian fluids. They consist of a flat plate and a rotating cone that measures the torque on the cone as a function of the rotational speed. The instrument uses this measurement of sheer to calculate the sample viscosity. Several rotational rates were used when taking viscosity measurements. At higher temperatures, higher rotational rates were used as the sample became more viscous. Taking the reciprocal of the viscosity yields fluidity, which can be graphed against the temperature to form a Fluidity Activation Plot.

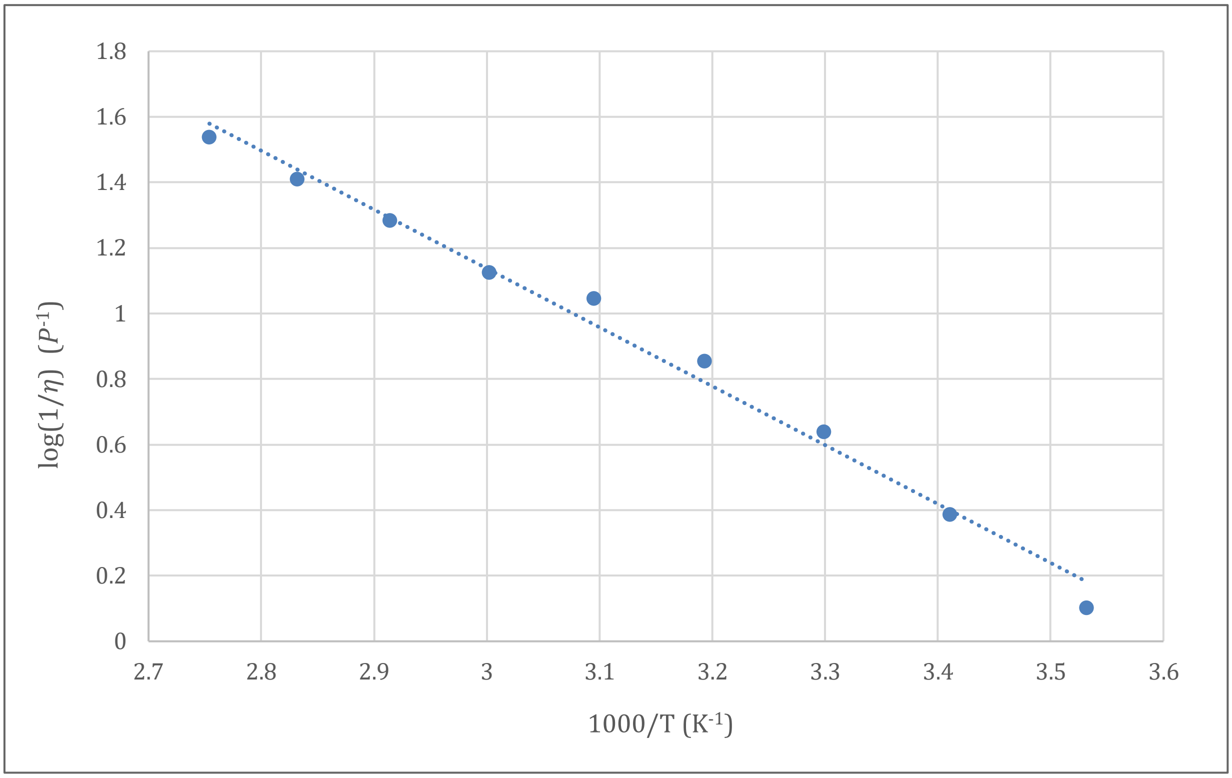

Figure 17. Fluidity Activation Plot for Me(PEG)$_3$-Im.

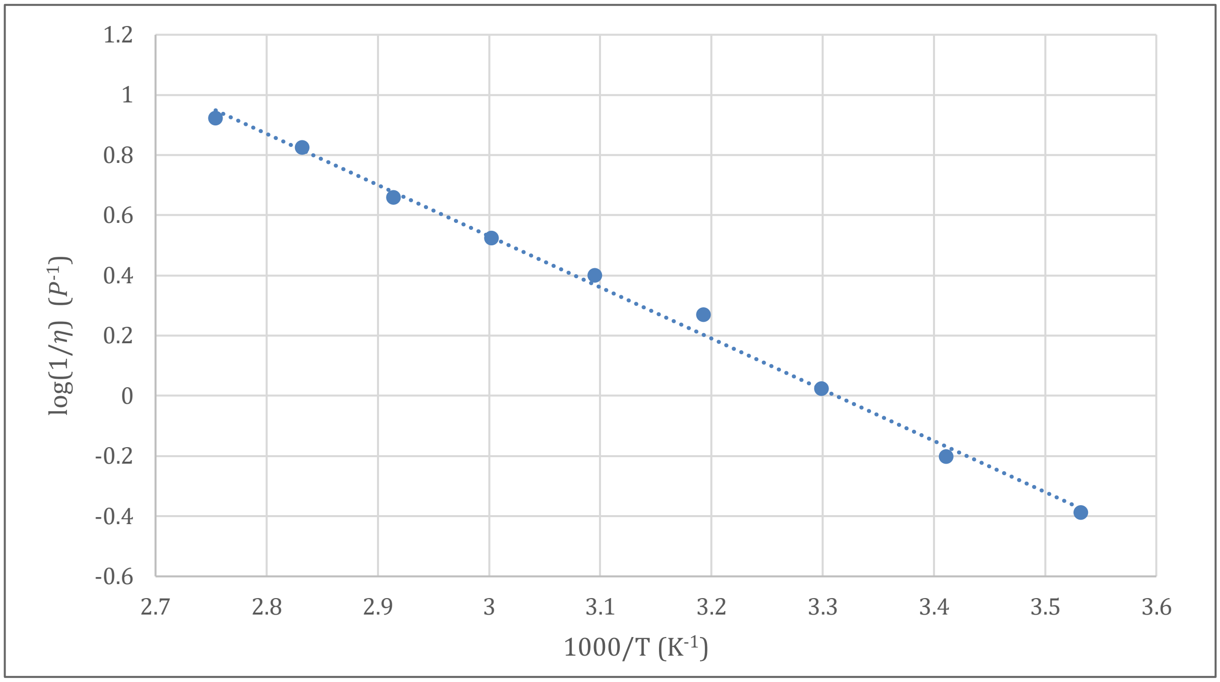

Figure 18. Fluidity Activation Plot for Me(PEG)$_7$-Im.

RESULTS AND DISCUSSION

Ionic Conductivity

Figures 15 and 16 show Arrhenius activation plots for ionic conductivity for the $MePEG_3$–Im^+ OH^- and $MePEG_7$–Im^+ OH^- polymer electrolytes synthesized from $MePEG_3OH$ and $MePEG_7OH$. Comparing the two polymer backbones, the longer PEG chain showed greater ionic conductivity at all temperatures measured. This behavior is counterintuitive to conventional polymer chemistry, but has been seen in many previous studies in our lab and in Murray's Lab.[8] This behavior is most likely due to the greater fluidity of the longer PEG chain, which increases the rate of rearrangement of the polymer electrolyte.

Interestingly, both of the PEG-based polymer electrolytes tested yielded higher conductivities than the H^+ conducting polymer electrolytes previously tested in our lab.[4,9] At 20° Celsius, the PEG_3 electrolyte showed a conductivity of 1.81×10^{-5} (S/cm) and the PEG_7 electrolyte showed a conductivity of 1.81×10^{-4} (S/cm).

Both values show fairly high conductivity; the ionic conductivity of a 0.1 mM KCl solution at this temperature was measure to be 3.80×10^{-3} (S/cm). The conductivity values increased with temperature as expected, because as an activation process, conductivity increases with increasing temperature according to the Arrhenius equation. These results also agree with the Stokes-Einstein and Nernst-Einstein equations which together predict that with an increase in fluidity, conductivity should also increase. This result will be further explored in the next section discussing fluidity. From the line of best fit, the equation obtained from the

PEG_3 polymer yielding an activation energy for ionic transport of 44.82 kJ/mol. This value was calculated using the Arrhenius relation shown in figure 16. This is a similar activation energy barrier to other H^+ conducting polymer electrolytes prepared in our laboratory, and is thought to be related to the activation barrier to rearrangement of the PEG segmental units. The activation energy calculated from the PEG_7 polymer data was 44.61 kJ/mol, which showed slightly greater mobility than the PEG_3 polymer. Due to having a similar activation energy as the previously measured H^+ conducting polymer electrolytes, we decided to compare fluidity vs temperature, as shown in Figure 17 and 18, in order to determine if the electrolyte was conducting ions via polymer segmental motion.

$$\sigma T = \sigma_o \exp\left(-\frac{E_a}{kT}\right)$$

Figure 19. Arrhenius relation for thermally activated conduction.

Viscosity

Viscosity measurements were obtained using a cone and plate viscometer, with viscosity measurements being given in centipoise (cP). Viscosity is a physical property that is dependent on temperature. Both electrolytes showed a decrease in viscosity with increasing temperature. The longer polymer chain was shown to be more viscous at all temperatures measured, both electrolytes followed a similar pattern as temperature was increased. The results of these measurements are shown in Figure 20 and 21 on a viscosity vs temperature plot.

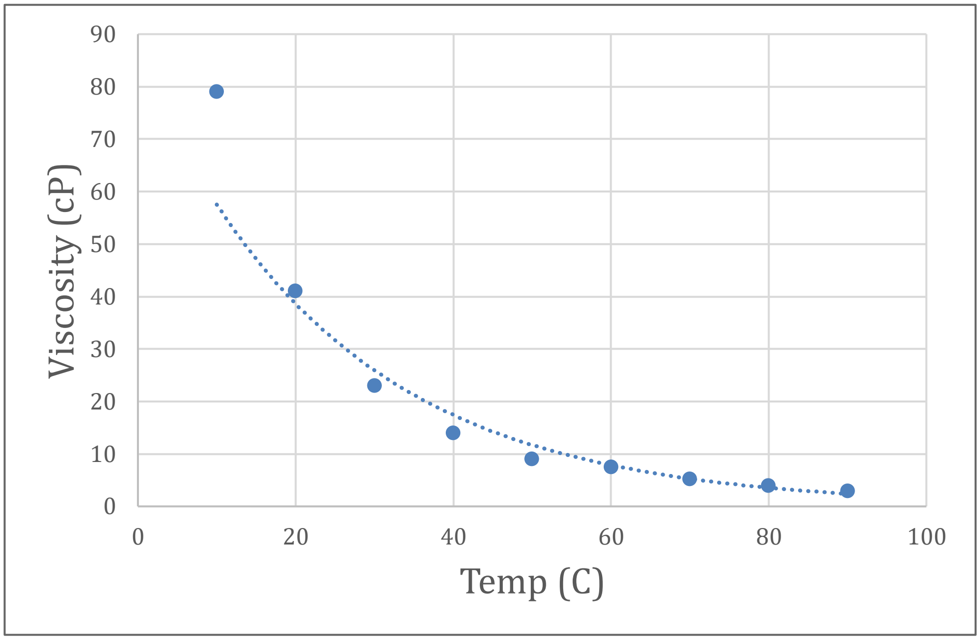

Figure 20. Viscosity vs Temperature plot for PEG3 based electrolyte.

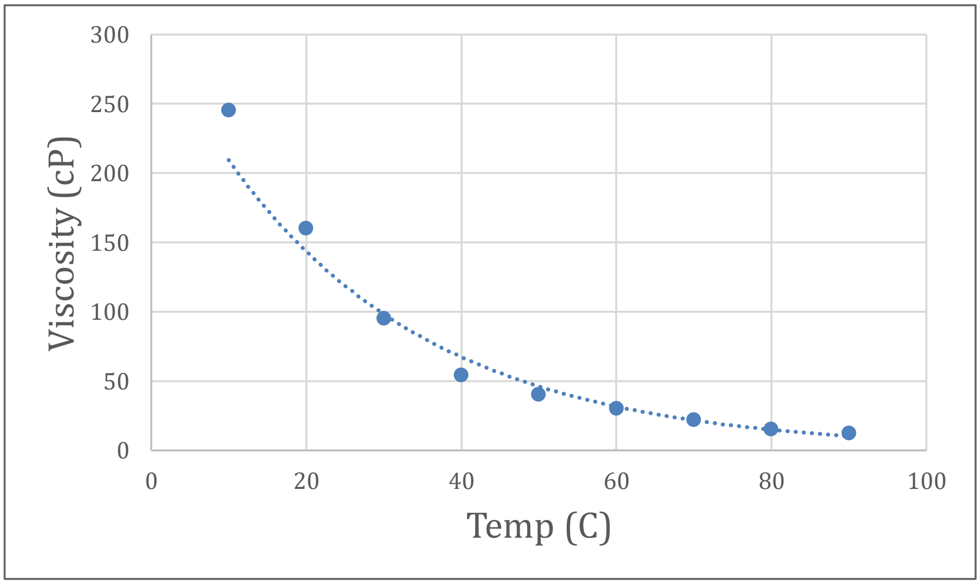

Figure 21. Viscosity vs Temperature plot for PEG7 based electrolyte.

The reciprocal value of viscosity is fluidity. Fluidity is the physical property of a substance that allows it to flow. At higher temperatures, both of the electrolytes showed the highest values of fluidity. This was also the case for ionic conductivity, which had the highest values at high temperatures. Therefore, it was shown that ionic conductivity increased with fluidity. The Stokes-Einstein equation (Figure 22) and the Nernst-Einstein equation (Figure 23) predicted that higher fluidity results in a larger ionic diffusion coefficient, and a higher ionic conductivity due to the increase in ionic mobility. This prediction held true during the experiments.

$$D = \frac{kT}{6\pi\eta R}$$

Figure 22. Stokes-Einstein Equation

$$\sigma_{\text{Ion}} = \frac{F^2}{RT}\left[z_+^2 D_+ C_+ + z_-^2 D_- C_-\right]$$

Figure 23. Nernst-Einstein Equation

Walden Plot

Figures 24 and 25 show Walden Plots (log molar equivalent conductivity vs. log fluidity) for both of the polymer electrolytes with a linear best fit applied. Using Angell's approximation of Walden plot data,[10] we understand that Walden Plots are good descriptors of ionic mobility in electrolytes with ion-ion interactions. That is, the Walden plot shows how the ionic mobility (molar equivalent conductivity) of a material increases as the fluidity of the material increases. As previously demonstrated, the ionic conductivity of a material should increase as the fluidity increases. The Walden plot is useful for determining the correspondence between the ionic mobility and fluidity.

The slope of a Walden Plot (α) is a value between 0 and 1 where 1 represents ideal behavior (fluidity and viscous drag are the only forces impeding ionic motion). If the value of the slope falls below 1, this indicates that factors other than viscosity impede ion mobility (i.e. the ionic conductivity is decreasing faster than the fluidity is decreasing). If the value is above 1, this indicates that the solution possibly shows superionic characteristics, and there may be a unique conductivity mechanism assisting the ionic mobility.

We constructed Walden plots with an "ideal" Walden line (α=1), shown in Figures 26 and 27, to compare with the data from both polymer electrolytes. Each point on a Walden plot corresponds to an independent measurement of both the ionic conductivity and viscosity of a polymer sample. If the data on the Walden plot lies on the ideal line, the material can be classified as a strong electrolyte. However, we have typically found that our H^+ conducting electrolytes fall below the ideal line, and we have understood this indicates that our acids are weak acids in the polymer medium.

The Walden data obtained from our measurements of conductivity and viscosity in our $MePEG_3$–Im^+ OH^- and $MePEG_7$–Im^+ OH^- polymer electrolytes is located within the lower left region of the Walden plot, which indicates either a weak electrolyte or the presence of ion-pairing in the electrolyte. Electrolytes in this region have an ionic conductivity that is much smaller than the ideal value of an electrolyte with the same viscosity. This means that there are factors negatively impacting the ionic conductivity other than viscosity and viscous drag on the mobile ions. Although the specific factors were not experimentally determined, the decreased conductivity could be due to ion pairing, or specific binding of the ions within the matrix. We plan to explore these factors in a future project.

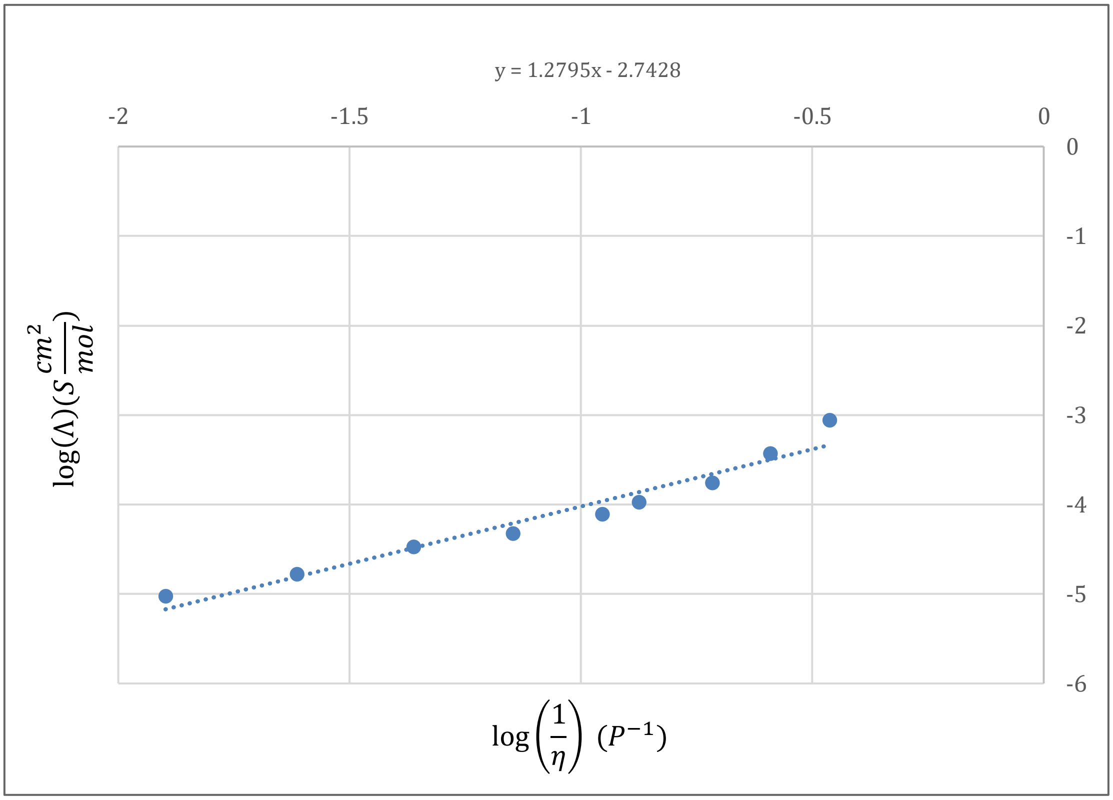

Figure 24. Walden Plot for PEG3 based electrolyte.

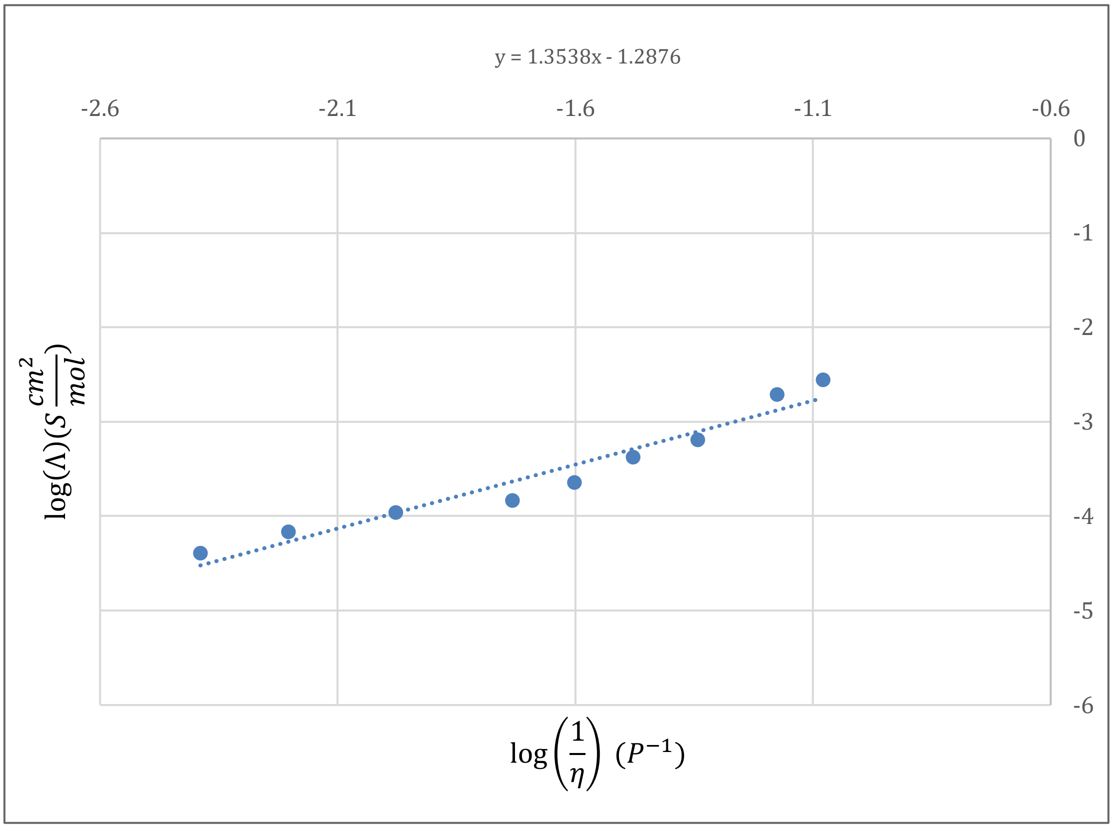

Figure 25. Walden Plot for PEG_7 based electrolyte.

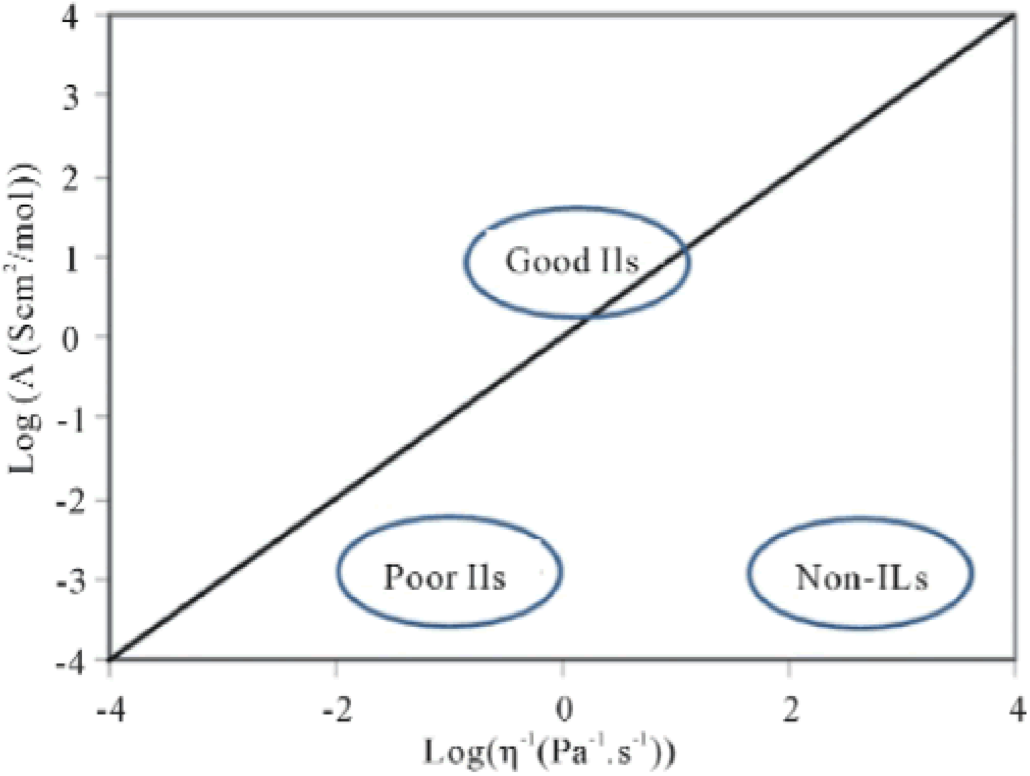

Figure 26. Example Walden Plot showing different ionic liquid regions. Figure Adapted from Reference.[11]

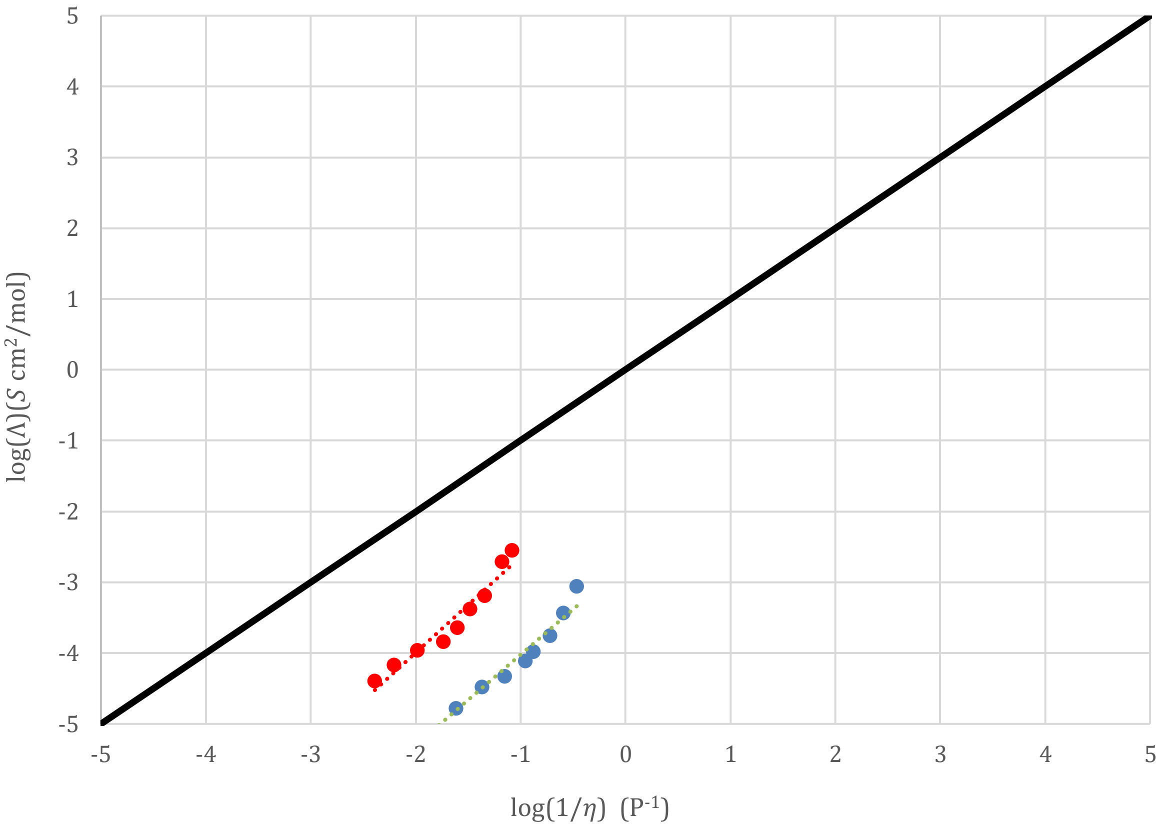

Figure 27. Walden Plot with PEG 7 (red) and PEG 3 (blue) compared to an "ideal" Walden line (black).

CONCLUSION

In this thesis, we have prepared two PEG-based hydroxide conducting polymer electrolytes differing in polymer lengths (MePEG$_3$ and MePEG$_7$) in order to study the ionic conductivity as a function of the structure of our polymer electrolytes. As we expected, the polymer with the greater fluidity showed a higher ionic conductivity. Interestingly, the larger MePEG$_7$ polymer had the largest fluidity and the largest ionic conductivity. This is atypical for polymers, as typically, the larger polymer has slower transport properties. However, we have found in our group that the concentration of free volume in a polymer greatly increases the transport properties in those polymers, and the MePEG$_7$ has a larger concentration of free volume than does the MePEG$_3$ polymer.

Through a comparison of the conductivity of the polymer electrolytes at various temperatures, we were able to quantitatively determine the activation energy for the ionic transport process. We also found that viscosity increases with MePEG$_n$ chain length which agrees with results from previous research.[5] The MePEG$_3$ and MePEG$_7$ both reached their highest conductivity values at 90 °C. These values were 4.54 x10^{-5} S/cm and 9.90 x10^{-5} S/cm, respectively. Graphs of the PEG electrolytes on a Walden plot gave results that were below the ideal Walden line, classifying the liquids as weak electrolytes.

REFERENCES

[1] D. Dekel, Alkaline membrane fuel cells, in Encyclopedia of Applied Electrochemistry, ed. R. Savinell, K.-I. Ota and G. Kreysa, Springer, Berlin/Heidelberg, SpringerReference number 303632

2 Bing-Ang Mei, Obaidallah Munteshari, Jonathan Lau, Bruce Dunn, and Laurent Pilon. "Physical Interpretations of Nyquist Plots for EDLC Electrodes and Devices" *The Journal of Physical Chemistry C,* 2018. *122* (1), pp. 194-206.

3 Ritchie, Jason E., and Jeffrey A. Crisp. "A Sol-Gel Synthesis of Polyether-Based Proton Conducting Electrolytes." Analytica Chimica Acta, vol. 496, no. 1-2, 2003, pp. 65-71.

4 Andrade, C. R. and Zaparoli, E. L., Effects of temperature-dependent viscosity on fully developed Laminar forced convection in a curved duct. International Communications in Heat and Mass Transfer, 28(2), pp. 211-220 (1985).

5 Giacomin, A. J., and P. H. Gilbert. "Exact-Solution for Cone-Plate Viscometry." *Journal of Applied Physics*, vol. 122, no. 17, 2017, pp. 175101.

6 Y.C. Wu, P.A. Berezansky, J. Res. Natl. Inst. Stand. Technol. 100 (1995) 521-527.

7 Y.C. Wu, W.F. Koch, J. Solution Chem. 20 (1991) 391-401.

8 Yancey, Benjamin, and Jason E. Ritchie. "Adding Free Volume to PEG Based Anhydrous Proton Conducting Electrolytes with Bulky Copolymers." *Journal of Electroanalytical Chemistry*, vol. 706, 2013, pp. 117-126.

9 Sun, Chengjun, and Jason E. Ritchie. "Star-Shaped MePEGnPolymers as H+Conducting Electrolytes." *The Journal of Physical Chemistry B*, vol. 115, no. 26, 2011, pp. 8381-8389.

10 W. Xu, E.I. Cooper, C.A. Angell. *The Journal of Physical Chemistry B*, 2003. 107, pp. 6170-6178

11 Ghandi, Khashayar. "A Review of Ionic Liquids, their Limits and Applications." *Green and Sustainable Chemistry*, vol. 4, no. 1, 2014, pp. 44-53.